

# Coherent Diffusive Photonics

Seabrata Mukherjee<sup>\*,1,†</sup> Dmitri Mogilevtsev<sup>\*,2,‡</sup> Gregory Ya. Slepyan,<sup>3</sup>  
Thomas H. Doherty,<sup>4</sup> Robert R. Thomson,<sup>1</sup> and Natalia Korolkova<sup>4</sup>

<sup>1</sup>*Institute of Photonics and Quantum Sciences, School of Engineering & Physical Sciences,  
Heriot-Watt University, Edinburgh, EH14 4AS, United Kingdom*

<sup>2</sup>*Institute of Physics, Belarus National Academy of Sciences, F. Skarina Ave. 68, Minsk 220072 Belarus*

<sup>3</sup>*Department of Physical Electronics, School of Electrical Engineering,  
Faculty of Engineering, Tel Aviv University, Tel Aviv 69978, Israel*

<sup>4</sup>*School of Physics and Astronomy, University of St Andrews,  
North Haugh, St Andrews KY16 9SS, United Kingdom*

The Photonic Circuit has generally been a structure in which light propagates by unitary exchange and where photons transfer reversibly between channels. In contrast, the term diffusive is more akin to a chaotic propagation in scattering media, where light is driven out of coherence towards a thermal mixture. We have devised a way to unite these opposites, founded from the dynamics of open quantum systems and resulting in novel techniques for coherent light control. The crucial feature of these photonic structures is dissipative coupling between modes; an interaction with a common reservoir. We demonstrate experimentally that such systems can perform optical equalisation to smooth multimode light, or act as a distributor, guiding it into selected channels. Quantum thermodynamically, these systems can act as catalytic coherent reservoirs by performing perfect non-Landauer erasure. When extending to lattice structures, localized stationary states can be supported in the continuum, similar to compacton-like states in conventional flat band lattices [1, 2].

The engineering of dissipation to a common reservoir generates a vast array of novel structures for photonic application and quantum simulation. It has already been shown that the coupling of a number of quantum systems to the same reservoir gives rise to a decoherence-free subspace of Hilbert space [3]. Moreover, evolution of the initial state towards this decoherence-free subspace is able to preserve and even create entanglement [4–7]. The careful engineering of loss can lead to coherence preservation [8–10], deterministic creation of non-classical states [11–13], and serve as a tool for quantum computation [14, 15]. Networks of dissipatively coupled systems can support topologically protected states [16]. In this Letter, we show both theoretically and experimentally that light can flow *diffusively* while remaining *coherent* and even entangled in a system of bosonic modes coupled to common reservoirs. Coherent diffusive light propagation opens new vistas for photonic applications, such as directional light distribution and diffusive equalisation. The coherent diffusive photonic circuits considered in this Letter are described by the following generic quantum master equation:

$$\frac{d}{dt}\rho = \sum_{j=1}^N \gamma_j \left( 2A_j \rho A_j^\dagger - \rho A_j^\dagger A_j - A_j^\dagger A_j \rho \right), \quad (1)$$

where  $\rho(t)$  is the density matrix and  $A_j$  denote the Lindblad operators for mode  $j$ . Quantities  $\gamma_j$  are relaxation rates into corresponding reservoirs. In the experiment,

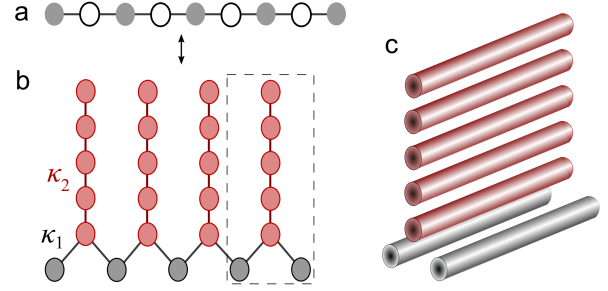


**Figure 1: 1D diffusive photonic circuit.** **a**, Dissipatively-coupled chain of the single mode waveguides. Every second waveguide (open circles) is lossy and serves as a reservoir. The waveguides indicated by closed circles exhibit low loss and couple dissipatively via these auxiliary waveguides only. **b**, Experimental realization of the chain in (a) using an integrated optical circuit. The lossy sites are implemented using auxiliary arrangements of coupled waveguides. Here  $\kappa_1$  is the coupling between chain modes and lossy sites and  $\kappa_2$  is the coupling between the waveguides forming the reservoirs. **c**, The three-dimensional geometry of the elementary diffusive circuit.

we use femtosecond laser inscribed [1, 17] arrays of coupled optical waveguides, where the propagation of the light can mimic the time evolution described by different Hamiltonians [18]. The relaxation rates  $\gamma_j$  describe then the coherence diffusion rate between neighbouring waveguides. Coupling to common reservoirs is realized by mutually coupling each pair of waveguides to a linear arrangement of further waveguides [19]; see Fig. 1.

Let us start with the simple example of 1D dissipatively coupled chain (*DiCC*) with  $A_j = a_j - a_{j+1}$ , where  $a_j$  ( $a_j^\dagger$ ) is the bosonic annihilation (creation) operator,  $a_j|\alpha_j\rangle =$

<sup>\*</sup>These authors contributed equally to this work.

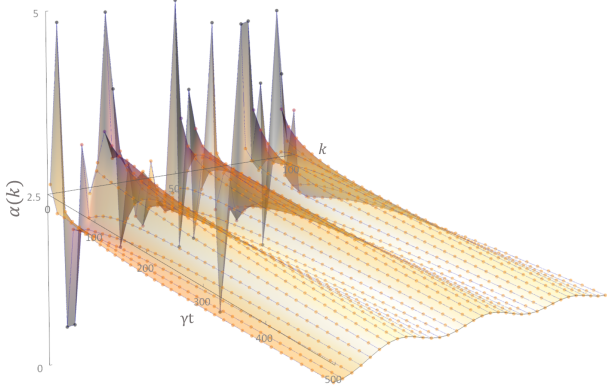


**Figure 2: Diffusive equalisation.** Amplitudes of the coherent states propagating through DiCC with equal coupling  $\gamma_j = \gamma$  as given by Eq. (1). The chain contains 100 modes. The initial random distribution in light amplitudes is smoothed out at the output demonstrating optical equalisation.

$\alpha_j |\alpha_j\rangle$ . Eq.(1) can then be recast in terms of coherent amplitudes  $\alpha_j$  (see Supplementary Material for details):

$$\frac{d}{dt} \alpha_k = -(\gamma_k + \gamma_{k-1})\alpha_k + \gamma_k \alpha_{k+1} + \gamma_{k-1} \alpha_{k-1}. \quad (2)$$

Eqs. (2) formally coincide with the equations of a time-dependent classical random walk in one dimension, the discrete analogue of diffusion and heat transport dynamics. However, there are no classical probabilities in Eqs. (1, 2), with the amplitudes  $\alpha_j$  being complex. While the light flows *diffusively*, like heat, its coherence is maintained: off-diagonal elements in the energy basis do not decay. For this to be the case, a fundamental role is played by the collective symmetrical superposition of all modes, characterized by a sum of modal operators:

$$A_{sum} = \sum_{j=1}^{N+1} \frac{a_j}{\sqrt{N+1}}. \quad (3)$$

If a state is not symmetrical over all modes, it follows from Eqs. (1, 2) that it will asymptotically decay to the vacuum state. Therefore, any state represented by a combination of operators  $A_{sum}$  and  $A_{sum}^\dagger$  is conserved by the dynamics of Eq. (3). These states can be quite diverse in nature, from highly non-classical to Gibbs states (see Supplementary Material). Furthermore, a stationary state can also be entangled: For a single photon in the DiCC, the state  $A_{sum}^\dagger \prod_{\forall j} |0\rangle_j$  is stationary [20].

Consider an initialization with all modal oscillators in coherent states. Eq. (1) shows that this will evolve into a product of coherent states with equal, averaged, amplitudes,  $\prod_{\forall j} |\alpha_{sum}\rangle_j$  where  $\alpha_{sum} = \sum_j \alpha_j / (N+1)$ . This feature of the diffusive, yet coherent 1D circuit, opens

the possibility to realise an optical equaliser, suppressing both intensity and phase fluctuations in multimode fields. The equaliser performance is illustrated in Fig. 1, where it is shown how the DiCC can completely smooth any arbitrary zero-mean variations of the input.

In order to realise engineered dissipative coupling in integrated waveguides in accordance with Eq. 1, one must be able to adiabatically eliminate lossy sites (Fig. 1a) from the system dynamics. This results in the fine tuning of the evanescent coupling parameters  $\kappa_{1,2}$ , where the coupling between chain modes and lossy sites,  $\kappa_1$ , must be considerably smaller than intra-reservoir couplings,  $\kappa_2$ . For the particular design of Fig. 1c,  $\kappa_1/\kappa_2 \approx 0.5$  should hold for all  $\gamma t$  (equivalently,  $\kappa_1 z$  in waveguide implementation, where  $z$  is the propagation distance along the chain waveguides). The length of the DiCC is not a prohibitive parameter and the collective behaviour, the coherent diffusive dynamics establishes itself already for merely two coupled bosonic modes. The effect of coherent optical equalisation can thus be readily achieved in the elementary circuit of Fig. 1c. In the experiment, a 30-mm-long elementary circuit with 20 waveguides in the reservoir was fabricated and the output intensity distribution was measured as a function of the wavelength,  $\lambda$ , of incident light. It should be mentioned that both  $\kappa_{1,2}$  vary linearly in the wavelength range of interest without affecting  $\kappa_1/\kappa_2$  significantly, and hence, wavelength tuning enables us to observe the dynamics as the effective analogous time,  $\kappa_1(\lambda)z$ , is tuned in this case. Fig. 3 depicts the corresponding experimental results, clearly demonstrating signal equalisation. In the next step, we fabricated a chain of five waveguides, coupled via similar reservoirs, and demonstrate the coherent diffusive equalising. We excited the central waveguide of the chain at the input and measured the intensity distribution after a propagation of  $z = 30$  mm. Fig. 4 shows the output intensities for three different values of  $\kappa_1 z$ . These experimental results are in good agreement with the numerically calculated output intensity distributions. Fig. 4 shows dynamically how the equalisation unfolds.

When the linear arrangement of modes in the DiCC is extended to further dimensions, a large vista of further applications becomes accessible. These range from re-routing photonic devices to simulators of many body quantum systems. Fig. 5a outlines a photonic circuit for which the excitation of two control modes can dissipatively direct a coherent flow of light (Fig. 5, b-d). This Quantum Distributor comprises two linear DiCC, connected by mutual interaction to the pair of control modes (See Supplementary Material). Here, the control modes perform the distribution catalytically, their coherence being conserved.

The simplest DiCC lattice structure comprises two linear chains placed parallel with dissipative connections between each neighbouring mode. This arrangement gives rise to the localization of signals which, unusually, is not

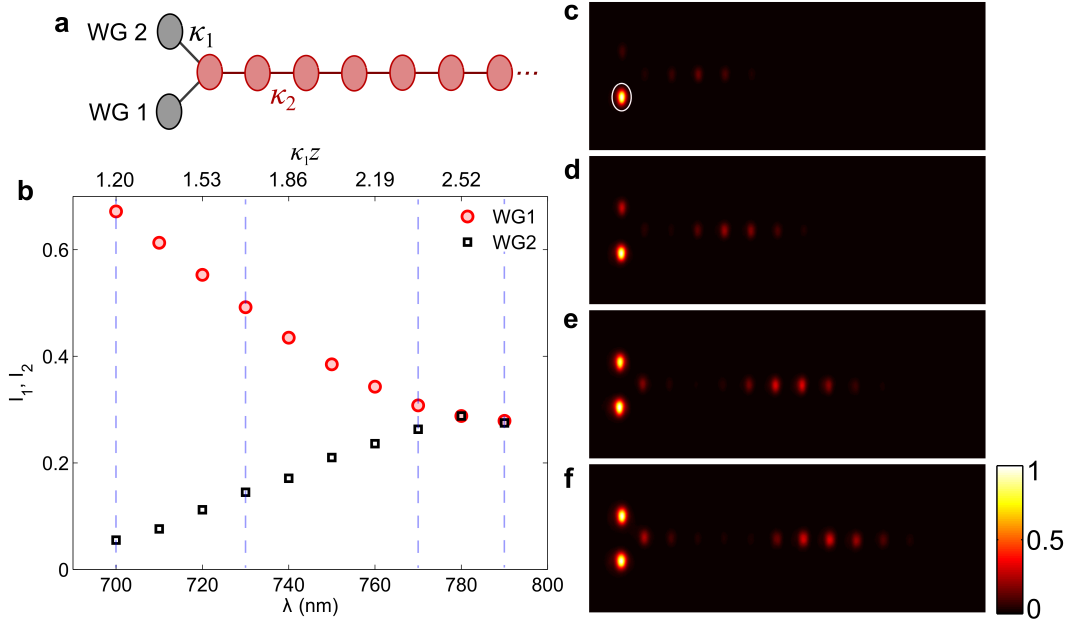


**Figure 3: Experimental observation of the coherent diffusive equalisation effect in a system of two dissipatively coupled waveguides.** **a**, Same as Fig. 1 c. WG1: waveguide 1, WG2: waveguide 2 - waveguides comprising the chain. Pink circles: a long chain of coupled waveguides which acts as the reservoir. The first waveguide in a reservoir chain is effectively a lossy site, which can be adiabatically eliminated to provide dissipative coupling between WG1 and WG2 (see also ref. [20]). **b**, The equalisation effect: initially, only WG1 is excited and the light intensities ( $I_{1,2}$ ) at WG 1,2 are measured after a propagation of  $z = 30$  mm. The coherent diffusive evolution distributes the input light equally between WG1 and WG2. In this implementation, the effective propagation time  $\gamma t$  of Eqs. (1) and Fig. 2 translates into propagation distance  $z$  along the grey waveguides in Fig. 1c. For a fixed sample length  $z$ , this dynamics is then best assessed by monitoring the output intensity as a function of the light wavelength as shown in the graph (see text and SM for details). This effectively corresponds to changing  $\gamma t \leftrightarrow \kappa_1 z$ . **c**, Output intensity distributions for four different wavelengths [700 nm, 730 nm, 770 nm and 790 nm, indicated by the vertical dashed lines in (b)].

borne of defects (see Supplementary Material). This is similar to the recently experimentally demonstrated lattice of unitarily coupled waveguides [1, 2]. An alternative circuit is a lattice of waveguides arranged in a honeycomb structure. The Lindblad operator for this system is  $L_j = \sum_{k=1}^6 (-1)^k a_{jk}$ , where  $j$  indexes hexagonal cells and  $k$  numbers the modes in the cell. If each mode in a hexagonal cell has same amplitude, the cell collectively constitutes a stationary, compacton-like, state. These states satisfy  $\langle L_j \rangle = 0, \forall j$ . It can be noted that they are robust with respect to additional losses in modes neighbouring the cell. If there are some losses within the stationary cell itself, some non-vacuum states can still be supported (Supplementary Material). Moreover, coherence can spread diffusively in the lattice.

Coherent diffusive dynamics of *DiCC* also has an intriguing quantum thermodynamical interpretation. For a long *DiCC* with identical initial coherent states of modes, the system will strongly equalise over any fluctuations. We then dissipatively couple one further ‘signal’ mode to this chain. This *DiCC* will act as a reservoir, driving the signal mode towards some state independent of its initial excitation, asymptotically disentangled from the remain-

der of the chain. The state of the *DiCC* after this interaction will belong to the same class of macro states as initially. Thus the long *DiCC* chain is acting as a catalytic reservoir to the signal mode, and forthwith we use the term reservoir to describe the arrangement.

Let us consider a *DiCC* with  $N + 1 \gg 1$  oscillators in coherent states, each of amplitude  $\alpha$ , and the dissipatively connected signal mode having amplitude  $a_0$ . For an arbitrary initial state of the  $a_0$  mode represented as  $\rho_{a0} = \sum_j p_j |\beta_j\rangle \langle \beta_j|_0$  [26], the stationary state

of the chain will be  $\rho_{st} = \sum_j p_j \prod_{k=0}^{N+1} |\bar{\alpha}_j\rangle \langle \bar{\alpha}_j|_k$ , with  $\bar{\alpha}_j = \frac{1}{N+2}(\beta + (N+1)\alpha_j)$ . For any finite set of  $\beta_j$ , the fidelity of the stationary state with the product of coherent states,  $|\Phi\rangle = \prod_{j=0}^{N+1} |\alpha_j\rangle_j$ , tends to unity for large  $N$ . A sufficiently long *DiCC* will therefore evolve any signal state into the coherent state initialized on the other oscillators in the chain. Hence the *DiCC* is indeed acting as a reservoir, washing away any information about the initial state. However, this clearly happens at a certain cost. The energy difference between the initial and

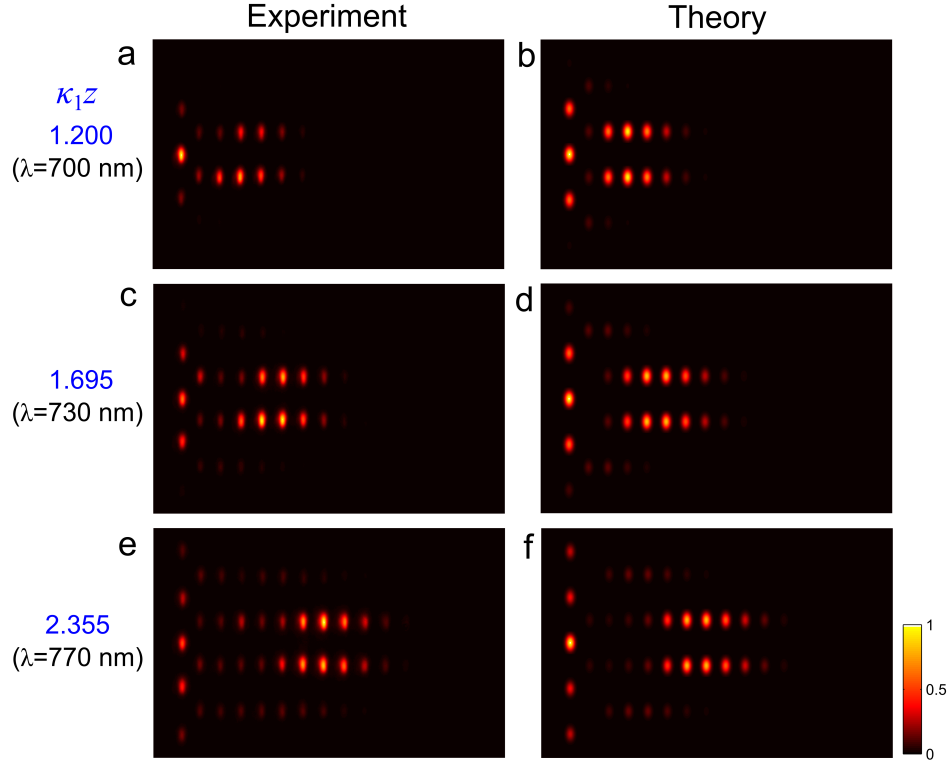


**Figure 4: Experimental observation of the coherent diffusive equalisation effect in a system of five dissipatively coupled waveguides.** Output intensity distributions for three different values of  $\gamma t \leftrightarrow \kappa_1 z$ . Here  $z = 30$  mm and  $\kappa_1$  was tuned by tuning the wavelength of incident light as in Fig. 3. The central waveguide was excited at the input for all measurements. In this device, the waveguides in the chain are coupled via identical reservoirs each containing 20 coupled waveguides.

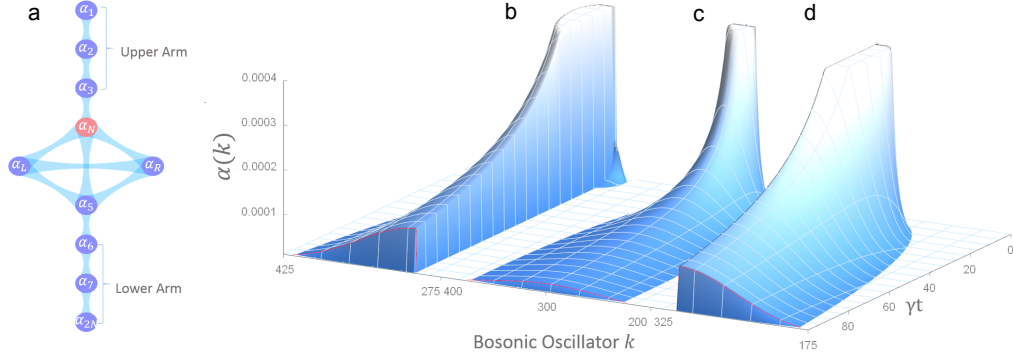


**Figure 5: Diffusive distribution** **a**, The simplest dissipative distributing structure with two arms; the number of waveguides,  $N = 600$ . **b**, Both control modes  $a_R$  and  $a_L$  are excited equally (or if both control modes are left in the vacuum state). Light is directed into the upper arm only. **c**, When the control mode  $a_L$  is excited initially, the excitation spreads equally into both arms. **d**, When the control modes are excited with opposite phases, light is guided to the lower arm.

asymptotic states of the chain and mode  $a_0$  is given by:

$$\Delta E = \frac{N+1}{N+2} \sum_j p_j |\beta_j - \alpha|^2. \quad (4)$$

Note that in the limit of large  $N$ , the energy balance of the mode  $a_0$  is the difference between the energies of the initial and the asymptotic state of the mode  $a_0$ :  $\Delta E_0 \approx$

$\sum_j p_j |\beta_j|^2 - |\alpha|^2$ . It can be equal to the energy lost of the whole mode  $a_0$  plus  $DiCC$  system, which holds for signal states satisfying  $|\alpha| = \sum_j p_j |\beta_j| \cos\{\arg(\beta_j) - \arg(\alpha)\}$ .

Therefore, erasure of the state of mode  $a_0$  can be performed without energy change of our reservoir. Such an action seems to contradict the famous Landauer's erasure principle: in order to erase information irreversibly,

by action of the environment, energy transfer into the environment need to occur [22]. However, this principle was formulated for classical systems. The quantum Landauer's principle holds under different assumptions. These consist of the reservoir being a closed, Gibbs state system, which is entirely uncorrelated with the signal state. If the reservoir is not isolated from the environment, the applicability of the Landauer's principle is questionable [23]. Indeed, the use of an additional quantum system coupled to the reservoir allows the state of the signal to be erased without entropic change. The *DiCC* is an example of the reservoir with such an additional quantum system.

In summary, we have illustrated novel possibilities for photonics that are generated by diffusive light propagation. The dissipative coupling of bosonic modes can allow light to flow like heat, whilst retaining coherence and even entanglement. A linear system of dissipatively coupled waveguides can act as an optical equaliser, smoothing fluctuations in amplitude and phase towards a common output. Non-classical input will evolve into a completely symmetrized, correlated, state of the whole system. This equalising action has been experimentally demonstrated in an elementary photonic circuit (Fig. 3) and for the chain of five waveguides (Fig. 4). Further, we have outlined dissipative circuits which can catalytically direct the flow of light across multiple channels, or even support stationary lattice states without impurity. In context of quantum thermodynamics, the *DiCC* itself can be considered as a reservoir with non-trivial properties. Remarkably, the state of the reservoir can remain unchanged throughout the process of interaction with an external, "signal" mode and allow non-Landauer erasure to be performed. Further, the optical equalisation and quantum evolution towards a stationary state can be used to study equilibration and thermalisation processes in quantum theory, one of the central problems in quantum thermodynamics [25]. In the future, we believe that diffusive photonic systems will find practical application both in studying the fundamental processes of structurally engineered open systems and in an array of integrated photonic technologies.

**Methods.** Arrays of coupled optical waveguides were fabricated using ultrafast laser inscription [17]. A 30-mm-long borosilicate substrate (Corning Eagle<sup>2000</sup>) was mounted on  $x$ - $y$ - $z$  translation stages (ABL1000). Each waveguide was fabricated by translating the stages once through the focus of the fs laser pulses generated by an Yb-doped fibre laser (Menlo Systems, BlueCut). The waveguide arrays were characterised using single-mode-fibre input coupling and free-space output coupling. To excite waveguides with tunable wavelength of light, a photonic crystal fibre [24] was pumped by sub-picosecond laser pulses of 1064 nm wavelength to generate a broad-band supercontinuum. A tunable monochromator placed after the supercontinuum source was used to select nar-

row band ( $\sim 3$  nm) light, which was coupled into an optical fibre (SMF-600). This fibre was then coupled to the lattice sites. The output intensity distribution was observed using a CMOS camera.

**Data availability statement.** Raw experimental data will be made available through Heriot-Watt University PURE research data management system (DOI: will be provided).

---

<sup>†</sup> Electronic address: [s.mukherjee@hw.ac.uk](mailto:s.mukherjee@hw.ac.uk)

<sup>‡</sup> Electronic address: [d.mogilevtsev@ifanbel.bas-net.by](mailto:d.mogilevtsev@ifanbel.bas-net.by)

- [1] Mukherjee, S., Spracklen, A., Choudhury, D., Goldman, N., Ohberg, P., Andersson, E., and Thomson, R. R., Observation of a Localized Flat-Band State in a Photonic Lieb Lattice., *Phys. Rev. Lett.* **114**, 245504 (2015).
- [2] Vicencio, R. A., Cantillano, C., Morales-Inostroza, L., Real, B., Mejia-Cortes, Cr., Weimann, S., Szameit, A., and Molina, M. I., Observation of Localized States in Lieb Photonic Lattices, *Phys. Rev. Lett.* **114**, 245503 (2015).
- [3] Palma, G.M., Suominen, K.-A., and Ekert, A.K., Quantum Computers and Dissipation, *Proc. Roy. Soc. London Ser. A* **452** 567 (1996).
- [4] Zanardi, P., and Rasetti, M., Noiseless Quantum Codes, *Phys. Rev. Lett.* **79** 3306 (1997).
- [5] Braun, D., Creation of Entanglement by Interaction with a Common Heat Bath, *Phys. Rev. Lett.* **89**, 277901 (2002).
- [6] Benatti, F., Floreanini, R., Piani, M., Environment Induced Entanglement in Markovian Dissipative Dynamics, *Phys. Rev. Lett.* **91**, 070402 (2003).
- [7] Lidar, D. A., Whaley, K. B., *Irreversible Quantum Dynamics*, Lecture Notes in Physics **622**, 83 (2003).
- [8] Carvalho, A. R. R., Milman, P., de Matos Filho, R. L., and Davidovich, L., Decoherence, Pointer Engineering, and Quantum State Protection, *Phys. Rev. Lett.* **86**, 4988 (2001).
- [9] Man, Z.-X., Xia, Y.-J., and Lo Franco, R., Cavity-based architecture to preserve quantum coherence and entanglement, *Sci. Rep.* **5**, 13843 (2015).
- [10] Man, Z.-X., Xia, Y.-J., and Lo Franco, R., Harnessing non-Markovian quantum memory by environmental coupling, *Phys. Rev. A* **92**, 012315 (2015).
- [11] Poyatos, J. F., Cirac, J. I., and Zoller, P., Quantum Reservoir Engineering with Laser Cooled Trapped Ions, *Phys. Rev. Lett.* **77**, 4728 (1996).
- [12] Ezaki, H., Hanamura, E., and Yamamoto, Y., Generation of Phase States by Two-Photon Absorption, *Phys. Rev. Lett.* **83**, 3558 (1999).
- [13] Clark, S., Peng, A., Gu, M., and Parkins, S., Unconditional Preparation of Entanglement between Atoms in Cascaded Optical Cavities, *Phys. Rev. Lett.* **91** 177901 (2003).
- [14] Verstraete, F., Wolf, M. M., and Ignacio Cirac, J., Quantum computation and quantum-state engineering driven by dissipation, *Nat. Phys.* **5**, 633 (2009).
- [15] Pastawski, F., Clemente, L., and Cirac, J. I., Quantum memories based on engineered dissipation, *Phys. Rev. A* **83** 012304 (2011).



- [16] Diehl, S., Rico, E., Baranov, M. A., and Zoller, P., Topology by dissipation in atomic quantum wires, *Nat. Phys.* **7**, 971 (2011).
- [17] Davis, K. M., Miura, K., Sugimoto, N., and Hirao, K., Writing waveguides in glass with a femtosecond laser, *Opt. Lett.* **21**, 1729 (1996).
- [18] Garanovich, I. L., Longhi, S., Sukhorukov, A. A., and Kivshar, Y. S., Light propagation and localization in modulated photonic lattices and waveguides, *Phys. Rep.* **518**, 1 (2012).
- [19] Biggerstaff, D. N., Heilmann, R., Zecevik, A. A., Grafe, M., Broome, M. A., Fedrizzi, A., Nolte, S., Szameit, A., White A. G., and Kassal, I., Enhancing coherent transport in a photonic network using controllable decoherence, *Nat. Comm.* **7**, 11282 (2016).
- [20] Mogilevtsev, D., Slepian, G. Ya., Garusov, E., Kilin, S., Korolkova, N., Quantum tight-binding chains with dissipative coupling, *New J. Phys.* **17**, 043065 (2015).
- [21] Rehacek, J., Mogilevtsev, D., and Hradil, Z., Operational Tomography: Fitting of Data Patterns, *Phys. Rev. Lett.* **105**, 010402 (2010).
- [22] Landauer, R., Irreversibility and Heat Generation in the Computing Process, *IBM J. Res. Dev.* **5**, 183-191 (1961); (reprinted in Leff & Rex (2003)).
- [23] Reeb, D., and Wolf, M. M., An improved Landauer principle with finite-size corrections, *New J. Phys.* **16** 103011 (2014).
- [24] Stone, J. M., and Knight, J. C., Visibly white light generation in uniform photonic crystal fiber using a microchip laser, *Opt. Express* **16**, 2670 (2008).
- [25] Gogolin, C., Eisert, J., Equilibration, thermalisation, and the emergence of statistical mechanics in closed quantum systems, *Rep. Prog. Phys.* **79**, 056001 (2016).
- [26] J. Rehacek, D. Mogilevtsev, and Z. Hradil, Operational Tomography: Fitting of Data Patterns, *Phys. Rev. Lett.* **105**, 010402 (2010).
- [27] Yu Guo and Heng Fan, A generalization of Schmidt number for multipartite states, *Int. J. Quantum Inform.* **13**, 1550025 (2015).

*Acknowledgements.* S.M. and R.R.T. sincerely thank the UK Science and Technology Facilities Council (STFC) for funding this work through ST/N000625/1. The authors acknowledge support from the EU projects FP7 People 2013 IRSES 612285 CANTOR (G.Ya.S.), Horizon-2020 H2020-MSCA-RISE-2014-644076 CoExAN (G.Ya.S.), and SUPERTWIN id.686731 (D.M.), the National Academy of Sciences of Belarus program “Convergence” (D.M.). T.D. and N.K. acknowledge the support from the Scottish Universities Physics Alliance (SUPA) and the Engineering and Physical Sciences Research Council (EPSRC). The project was supported within the framework of the International Max Planck Partnership (IMPP) with Scottish Universities. D.M. is thankful to Dr. V. Shatokhin for useful discussions.

*Author contributions.* D.M., G.Ya.S. and N.K. conceived the theory, S.M. and R.R.T. devised the experiment, S.M. designed, fabricated and characterized the photonic devices, T.D., D.M. and S.M. carried out theoretical calculations, D.M., S.M. and N.K. wrote the manuscript.

N.K. and R.R.T. supervised the project, all authors discussed the paper.

*Competing Interests.* The authors declare that they have no competing financial interests.

*Correspondence* Correspondence and requests for materials should be addressed to

S.M. (email: [s.mukherjee@hw.ac.uk](mailto:s.mukherjee@hw.ac.uk)) and

D.M. (email: [d.mogilevtsev@ifanbel.bas-net.by](mailto:d.mogilevtsev@ifanbel.bas-net.by)).

### Supplementary Note 1: Experimental model

The coherent diffusive photonic circuits considered in this Letter are described by the following generic quantum master equation:

$$\frac{d}{dt}\rho = \sum_{j=1}^N \gamma_j \left( 2A_j \rho A_j^\dagger - \rho A_j^\dagger A_j - A_j^\dagger A_j \rho \right), \quad (\text{S1})$$

where  $\rho(t)$  is the density matrix and  $A_j$  denote the Lindblad operators for mode  $j$ . Quantities  $\gamma_j$  are relaxation rates into corresponding reservoirs describing the coherence diffusion rate between neighbouring waveguides. This time evolution is modelled in the experiment by the arrays of coupled optical waveguides. The reservoirs are realized by mutually coupling each pair of waveguides to a linear chain of further waveguides as shown in Fig. S1. Interesting feature of the behaviour of light in these devices is the interchangeability between propagation distance and wavelength. The effective time of evolution  $\gamma t$  can be altered both by changing the length of the waveguide block, or the wavelength of light incident upon it. As the wavelength is tuned,  $\kappa_1$  changes almost linearly to keep  $\kappa_1/\kappa_2 \approx 0.5$ , maintaining the correct character of dynamics.

Notice that the dependence of diffusion rates,  $\gamma_j$ , on time does not change neither the diffusive character of the dynamics nor the asymptotic state provided that always  $\gamma_j(t) > 0$ .

### Supplementary Note 2: Measurement of evanescent coupling

As mentioned in the main text, the control of evanescent coupling is crucial for the experimental realisation of the diffusive equaliser. In Fig. S2 we present the measured variation of  $\kappa_{1,2}$  as a function of the wavelength of incident light,  $\lambda$ . We fabricated two types of directional couplers (each consisting of two evanescently coupled straight waveguides) which are the building blocks of the photonic circuits shown in Fig. S1. For the first type, where the two waveguides are at 45° angle, the coupling constant is  $\kappa_1$  and that for the second type (consisting of

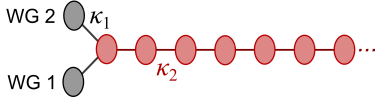


**Figure S1:** Elementary photonic circuit. Values and, even more, ratio of evanescent couplings  $\kappa_1$  (chain-reservoir) and  $\kappa_2$  (inter-reservoir) are crucial for the validity of the model.

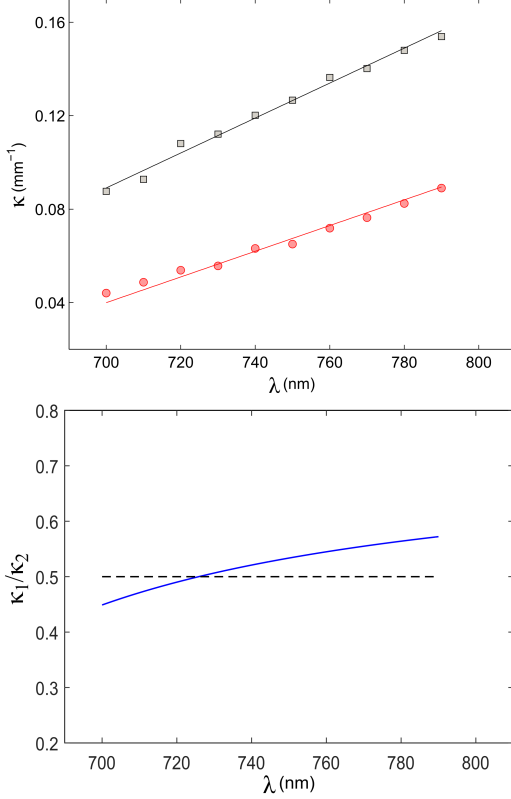


**Figure S2:** (Upper) Variation of coupling constants ( $\kappa_1 \rightarrow$  red and  $\kappa_2 \rightarrow$  black) as a function of wavelength of light. The solid lines are linear fits. (Lower) Variation of  $\kappa_1/\kappa_2$  as a function of wavelength of light. In the wavelength range of interest (i.e. 700-780 nm), this remains very close to the desired value of 0.5 (dashed line) with a maximum deviation of  $\approx \pm 0.05$ .

two horizontally separated waveguides) is  $\kappa_2$ . Measuring the light intensities at the output of these 30-mm-long directional couplers, we calculated  $\kappa_{1,2}(\lambda)$ . It was observed that for these couplers, the ratio of  $\kappa_{1,2}$  remains very close to the desired value of 0.5 with a maximum deviation of  $\approx \pm 0.05$ .

### Supplementary Note 3: Dynamics of the dissipatively coupled bosonic chain

Due to linearity of Eq. (S1), the initial coherent states propagation through DiCC remain coherent states at any time moment of dynamics described by Eq. (S1). Con-

sider the Glauber  $P$ -function for the density matrix,  $\rho(t)$ , of the state describing the circuit:

$$\rho(t) = \int d^2\vec{\alpha} P(\vec{\alpha}, \vec{\alpha}^*; t) |\vec{\alpha}\rangle \langle \vec{\alpha}|,$$

where  $|\vec{\alpha}\rangle = \prod_j |\alpha_j\rangle$ ;  $|\alpha_j\rangle$  is the coherent state of  $j$ -th mode of the circuit and the amplitude  $\alpha_j$  represents the  $j$ -th elements of the vector  $\vec{\alpha}$ . For the DiCC with  $N+1$  modes and  $j$ th Lindblad operator represented as  $A_j = a_j - a_{j+1}$ , the solution for the  $P$ -function is obtained from the following Fokker-Planck equation:

$$\frac{\partial}{\partial t} P(\vec{\alpha}, \vec{\alpha}^*; t) = \left( \sum_{j=1}^N \gamma_j \left( \frac{\partial}{\partial \alpha_j} \alpha_j - \frac{\partial}{\partial \alpha_j} \alpha_{j+1} - \frac{\partial}{\partial \alpha_{j+1}} \alpha_j + \frac{\partial}{\partial \alpha_{j+1}} \alpha_{j+1} \right) + \text{h.c.} \right) P(\vec{\alpha}, \vec{\alpha}^*; t)$$

Due to linearity of this equation the solution can be represented as  $P(\vec{\alpha}, \vec{\alpha}^*; t) = P(\vec{\alpha}(t), \vec{\alpha}^*(t))$ , where dynamics of amplitudes is described by Eqs. (2) of the main text. It is instructive to represent the initial state in terms of discrete superposition of coherent state projectors [26]:

$$\rho(0) = \sum_{\forall k} p_k \prod_{\forall j} |\alpha_{jk}\rangle \langle \alpha_{jk}|_j, \quad (\text{S2})$$

where the index  $k$  labels a set of amplitudes  $\{\alpha_{k1}, \alpha_{k2}, \dots\}$ . The time-dependent Glauber function corresponding to the initial state (S2) is given by Eq. (S1) as

$$P(\vec{\alpha}, \vec{\alpha}^*; t) = \sum_{\forall k} p_k \prod_{\forall j} \delta(\alpha_j - \alpha_{jk}(t)) \delta(\alpha_j^* - \alpha_{jk}^*(t)),$$

where amplitudes  $\alpha_{jk}(t)$  for the DiCC are defined from Eq. (2) of the main text.

As follows from Eq. (S1), any density matrix which is function of operators  $A_{\text{sum}} = \sum_{j=1}^{N+1} \frac{a_j}{\sqrt{N+1}}$ ,  $A_{\text{sum}}^\dagger$ , and the vacuum,  $\rho_{\text{vac}} = \prod_{\forall j} |0\rangle \langle 0|_j$ , corresponds to a stationary state. These states can be of a quite different nature. The stationary state can be just the pure product of coherent states of individual modes with the same amplitude:

$$\rho_{st} = |\Phi_{st}\rangle \langle \Phi_{st}|, \quad |\Phi_{st}\rangle = \prod_{\forall j} |\alpha_j\rangle. \quad (\text{S3})$$

However, it can also be quite exotic, for example, it can be a Schrödinger-cat entangled state with  $|\Phi_{st}\rangle \propto \sum_{k=1}^K w_k \prod_{\forall j} |\alpha_k\rangle_j$ , where  $K$  is the number of different components in our cat-state and  $w_k$  are scalar weights. The Gibbs state

$$\rho_{st} = \frac{\exp\{-\beta A_{\text{sum}}^\dagger A_{\text{sum}}\}}{\text{Tr}\{\exp\{-\beta A_{\text{sum}}^\dagger A_{\text{sum}}\}\}} \quad (\text{S4})$$

also belongs to the stationary states of the system. This state has maximal entropy for the given sum of the second-order coherences,  $\langle a_k^\dagger a_l \rangle$  (which is also conserved by the dynamics). As was already mentioned, the stationary state can also be maximally entangled.

The DiCC evolves toward stationary state in a quite remarkable way. The initial state of the DiCC with  $N + 1$  modes corresponding to the coherent state of all the chain modes,  $|\Phi_0\rangle = \prod_j |\alpha_j\rangle_j$ , evolves to the product of coherent states with equal amplitudes,  $|\Phi_{t \rightarrow \infty}\rangle = \prod_j |\alpha_{sum}\rangle_j$ , where the amplitude is the averaged sum of all the amplitudes,  $\alpha_{sum} = \sum_j \alpha_j / (N + 1)$ . Then an arbitrary initial state of the DiCC (S2) will be asymptotically reduced to the following form:

$$\rho_{st} = \sum_{\forall k} p_k \prod_{j=1}^{N+1} |\bar{\alpha}_k\rangle \langle \bar{\alpha}_k|_j \quad (\text{S5})$$

with  $\bar{\alpha}_k = \frac{1}{N+1} \sum_{j=1}^{N+1} \alpha_{jk}$ . Actually, the DiCC drives the initial state to the symmetrical state over all the modes. Note, that the smoothing action of DiCC is preserved even for the case of different decay rates,  $\gamma_j \neq 0$ . Stationary states do not depend on them.

#### Supplementary Note 4: Distributor structure

The prerequisite of the distributing action considered here is the existence of several localised stationary states of the structure described by the master equation Eq. (S1). For simplicity sake, we consider here pure stationary states. We call the state  $|\chi^{loc}\rangle$  "localised" if exists some subset,  $\{m\}$ , of  $M < K$  systems of our dissipatively coupled photonic circuit such that  $\sum_{k \in \{m\}} \langle \chi^{loc} | a_k^\dagger a_k | \chi^{loc} \rangle > 0$ ,

whereas for systems out of the subset  $\{m\}$  we have  $\sum_{k \notin \{m\}} \langle \chi^{loc} | a_k^\dagger a_k | \chi^{loc} \rangle = 0$ . The most simple and obvious distributing action would be possible if the initial state of the structure,  $\rho_0$ , is orthogonal to some localised stationary state,  $\langle \chi_j^{loc} | \rho_0 | \chi_j^{loc} \rangle = 0$ . Then the part of the structure corresponding to subset  $\{m_j\}$  will not be excited in the process of dynamics described by Eq. (S1). For such a distributor to be non-trivial, sets corresponding to different localised states,  $\{m_j\}$ , have to be partially overlapping. Distributor can be realized even in the case when the localised stationary states corresponding to different parts of the structure are not mutually orthogonal. Let us illustrate our consideration with the example of the slightly modified DiCC. For the structure depicted in Fig. 5a of the main text, modes in the arms are coupled pairwise,  $A_j = a_j - a_{j+1}$  for  $j = 1 \dots N-1, N+2 \dots 2N$ . For the central controlling node  $L_N = a_N - a_H + a_L -$

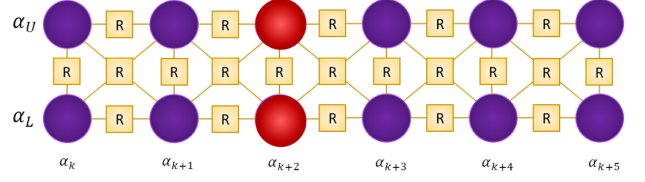


**Figure S3:** 2D photonic circuit: double chain. R: reservoirs. Circles - bosonic modes (red labels one of the possible initial excitation).

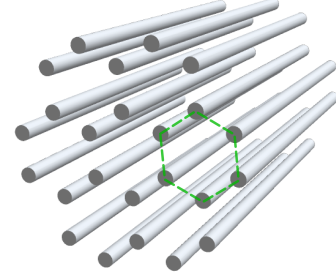


**Figure S4:** Bosonic modes arranged in a honeycomb lattice can lead to compacton-like localised states. The dashed like indicates the localised state.

$a_{N+1}$ . From the master equation Eq. (S1), the equation similar to Eq. (2) of the main text can be obtained for each arm. For four modes of the central node the equations are as follows:

$$\begin{aligned} \frac{d}{dt} \alpha_N &= -(\gamma_N + \gamma_{N-1}) \alpha_N + \gamma_{N-1} \alpha_N + \gamma_N (\alpha_{N+1} + \alpha_H - \alpha_L), \\ \frac{d}{dt} \alpha_H &= -\gamma_N (\alpha_H - \alpha_N + \alpha_{N+1} - \alpha_L), \\ \frac{d}{dt} \alpha_L &= -\gamma_N (\alpha_L + \alpha_N - \alpha_{N+1} - \alpha_H), \\ \frac{d}{dt} \alpha_{N+1} &= -(\gamma_N + \gamma_{N+1}) \alpha_{N+1} + \gamma_{N+1} \alpha_{N+2} + \gamma_N (\alpha_{N+1} - \alpha_H + \alpha_L). \end{aligned} \quad (\text{S6})$$

These equations describe 1D classical random walk. So, stationary states for arms decoupled from the central node would be vectors with equal elements,  $\alpha_j = \alpha$  for  $j = 1 \dots N$  or  $j = N + 1 \dots 2N$  and arbitrary  $\alpha$ . Also, there is a stationary state localised in two controlling modes,  $a_H$  and  $a_L$ , with  $\alpha_H = \alpha_L$  and  $\alpha_j = 0$ ,  $j = 1 \dots 2N$ . Obviously, for the whole structure the equal distribution of amplitudes in both arms  $\alpha_j = \alpha$  for  $j = 1 \dots N$  and  $j = N + 1 \dots 2N$ , and equal amplitudes in the controlling modes,  $\alpha_H = \alpha_L$  is also the stationary state. Excitation of just one arm and one of the controlling modes with equal amplitudes (i.e., for example,  $\alpha_j = \alpha$  for  $j = 1 \dots N$ ,  $\alpha_H = \alpha$  and  $\alpha_L = 0$ ,  $\alpha_j = 0$  for  $j = N + 1 \dots 2N$ ) is also a stationary state. By exciting control modes,  $a_H$  and  $a_L$  in certain states,



one can make an initial excitation of a particular mode propagate either to the one arm, or to another, or to both arms simultaneously (see Fig. 5). Notice, the such a distributing action can be achieved *catalytically*, since, as it follows from Eqs.(S6), the coherence of two controlling modes are conserved,  $\alpha_H(t) + \alpha_L(t) = \alpha_H(0) + \alpha_L(0)$ , for any time-moment,  $t$ . In Fig. 5 (b-d) one can see an illustration of the distribution for the two-arm structure shown in Fig. 5a.

### Supplementary Note 5: Double chain and dissipative localization

Here we consider a simple generalization of the DiCC for the case of two parallel dissipatively coupled DiCC (Fig S3). Our chain consists of squares connected by sides, so, the Lindblad operator of  $j$ -th square is

$$A_j = a_{j,+} - a_{j,-} + a_{j-1,+} - a_{j-1,-}. \quad (\text{S7})$$

We obtain the following set of equations for the coherent amplitudes:

$$\frac{d}{dt}\vec{\alpha}_j = -\gamma\hat{O}(2\vec{\alpha}_j - \vec{\alpha}_{j-1} - \vec{\alpha}_{j+1}), \quad (\text{S8})$$

where the matrix  $\hat{O}$  has elements  $\hat{O}_{j,k} = (-1)^{j+k}$ ,  $j, k = 1, 2$ . The vector  $\vec{\alpha}_j = [\alpha_{j,+}, \alpha_{j,-}]^T$ . Despite being only a slight modification of the simplest DiCC, the doubled chain has a number of drastically different features. First of all, any vector of coherent amplitudes,  $\vec{\alpha}_j$ , with equal upper (+) and lower (-) components is the stationary localised state. Then, initial excitation of any lattice site (say,  $\alpha_{j,+} = x$ ) gives rise to the stationary state consisting of two-site localised state  $\alpha_{j,+} = \alpha_{j,-} = x/2$  plus delocalised state  $\alpha_{k,+} = (-1)^{j-k}x/2N$ ,  $\alpha_{k,-} = (-1)^{j-k+1}x/2N$ , where  $N$  is the number of systems in each chain. It is interesting that the double chain can serve as an analogous filter. If both the lower and upper chains is excited, the stationary result in each site would be half of the sum of the lower and upper initial amplitudes. Also, localised states are robust. Additional losses on sites out of the localisation region do not affect the localised states. However, they do affect the de-localised stationary states driving them to the vacuum.

Such localisation phenomena can hold also for infinite perfectly periodic dissipatively coupled photonic lattices. Let us assume Lindblad operators of the following form

$$A_j = \sum_{k \in \{n_j\}} x_{jk} a_k. \quad (\text{S9})$$

where  $\{n_j\}$  denotes a set of modes coupled to the same dissipative reservoir;  $x_{jk}$  are scalar weights describing such a coupling. To avoid trivial localised states, we assume that there are no isolated sets, and for any  $\{n_j\}$  there is a set  $\{n_l\}$  such that the intersection,  $\{n_j\} \cap \{n_l\}$ ,

$j \neq l$ , is not empty, but unequal to any of  $\{n_j\}$ . Additionally, for the ideally periodic structures we assume that any operator,  $a_k$ , belongs to at least two different sets, and any set transforms to other set by translation along lattice vectors,  $\vec{e}_i$ . Obviously, for any localised stationary state we have  $A_j \rho^{loc} = 0 \forall j$ . From Eq. (S9) it follows that any localised state occupies at least two sites of the structure. An example of the honeycomb lattice allowing for dissipative localisation is shown in Fig. S4 and briefly discussed in the main text.

To demonstrate basic features of dissipative localisation, let us consider here a simple example of square lattice (see insets in Fig. S5). Denoting the sites in the upper left corner of each square as  $(j, k)$ , we obtain the following Lindblad operators for such a lattice:

$$A_{j,k} = a_{j,k} + a_{j+1,k} + a_{j,k+1} + a_{j+1,k+1}. \quad (\text{S10})$$

The equations for the amplitudes Eqs.(1, S10) then read:

$$\begin{aligned} \frac{d}{dt}\alpha_{j,k} &= -\gamma_{j,k}\langle A_{j,k} \rangle - \gamma_{j+1,k+1}\langle A_{j+1,k+1} \rangle, \\ \frac{d}{dt}\alpha_{j+1,k} &= -\gamma_{j,k}\langle A_{j,k} \rangle - \gamma_{j+1,k-1}\langle A_{j+1,k-1} \rangle. \end{aligned} \quad (\text{S11})$$

As seen from Eqs. (S11), the minimal localised states for an infinite square lattice of Fig. S5 involve at least four sites ( for example, the localized state can be in the set  $\{m\} = \{(j+1, k), (j+2, k), (j+1, k+1), (j+2, k+1)\}$ ). An example of the localised state composed of coherent states is

$$\begin{aligned} |\Psi^{loc}\rangle &= |\alpha\rangle_{j+1,k} - |\alpha\rangle_{j+2,k} \\ &+ |\alpha\rangle_{j+2,k+1} - |\alpha\rangle_{j+1,k+1} \prod_{j,k \notin \{m\}} |0\rangle_{j,k}. \end{aligned} \quad (\text{S12})$$

Any closed contour including either 0, 2 or 4 sites of every square can host a localised state. A finite lattice can support also localised edge states not only of even, but also of odd number of sites. For example, the three-site edge state in the upper left corner of the lattice shown in the inset of Fig. S5 can have coherent state with amplitude  $2\alpha$  in  $(1, 1)$  and states with the amplitudes  $-\alpha$  in sites  $(2, 1)$  and  $(1, 2)$ .

Localised states of a dissipatively coupled lattice can be arbitrarily extended. A state can propagate through the lattice exciting localised states in several cells. To illustrate the basic features of such propagation, let us consider the dynamics of just a single unit cell of the square lattice (just one  $A_{j,k}$  of Eq. (S10)). One has

$$\vec{a}(t \rightarrow \infty) = (1 - \mathbf{S}/4)\vec{a}(0), \quad (\text{S13})$$

where the vector of time-dependent modal amplitudes is  $\vec{a}(t) = [\alpha_{1,1}(t), \alpha_{1,2}(t), \alpha_{2,1}(t), \alpha_{2,2}(t)]^T$  and  $\mathbf{S}$  is the unit matrix. Eq. (S13) shows that the final result is an initial state minus the result of complete symmetrisation of it over the cell. Similar process occurs for the

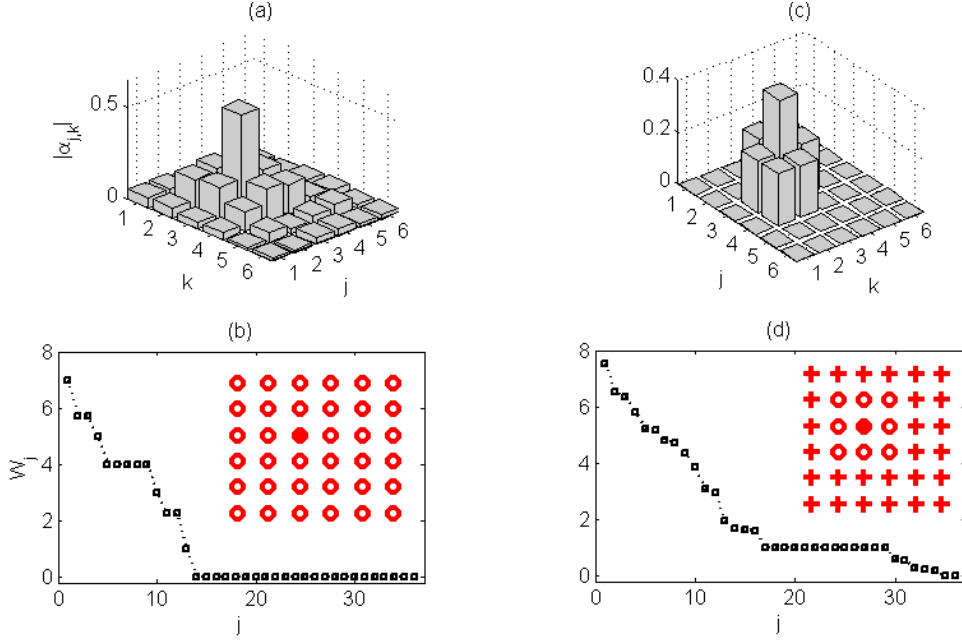


**Figure S5:** Stationary distributions of absolute values of modal amplitudes for  $6 \times 6$  square lattice in absence of additional losses (a) and for additional losses (c) in sites of the lattice denoted by crosses in the inset of the panel (d). Panels (b, d) show eigenvalues (in the units of  $\gamma$ ) of the system (S11) without additional losses (b) and with additional losses (d). Filled dots in the insets on (b, d) show a position of the initial excitation.

complete lattice. Symmetrical parts propagate. Curiously, this process is described by the classical two-dimensional random walk. Let us introduce variables  $\lambda_{m,n}(t) = (-1)^{m+n} \langle A_{m,n}(t) \rangle$ . For  $\gamma_j \equiv \gamma > 0, \forall j$ . From Eqs. (S11) it follows that

$$\frac{d}{dt} \lambda_{m,n} = -4\gamma \lambda_{m,n} + \gamma (\lambda_{m+1,n} + \lambda_{m-1,n} + \lambda_{m,n+1} + \lambda_{m,n-1}).$$

Similar heat-like propagation of coherences was found recently in dissipatively coupled 1D spin chains [20]. An illustration of the stationary distribution arising from the initial excitation of just one mode is given in Fig. S5(a). In Fig. S5(b) a spectrum of the equation matrix for Eqs. (S11) is given. The plateau of zero eigenvalues are separated from the non-zero eigenvalues with the gap of  $\gamma$ . Eq. (S14) points also to the existence of delocalised stationary modes given by the condition  $\langle A_{m,n} \rangle = (-1)^{m+n} \alpha$ .

Despite coupling to neighbor sites, the stationary localised state is completely impervious to additional loss even on sites adjacent to those where the stationary state is localised. It can be seen even for the simplest example of the single-cell system. Taking the equation matrix (S10) with two sites subjected to additional loss with the rate  $\gamma$  as  $-\gamma(\mathbf{S} - \text{diag}(1, 1, 0, 0))$ , one gets  $\vec{a}(t \rightarrow \infty) = \mathbf{O} \vec{a}(0)$ , where the only non-zero elements of the matrix  $\mathbf{O}$  are  $O_{3,3} = O_{4,4} = 0.5$  and  $O_{3,4} = O_{4,3} = -0.5$ . Again,

the result is the initial vector minus its symmetrisation, but only for the modes untouched by the additional loss. Similar effect holds for a larger lattice. In Fig. S5(c) one can see an example of localised state in the region free of additional loss arising from the initial excitation of just one initial mode. The inset in the panel Fig. S5(d) shows sites affected by additional individual loss with rate  $\gamma$ . Fig. S5(d) shows eigenvalues of the equation matrix Eqs. (S11) for this case. Only two localised states survive for the case, and the gap between the zero plateau and decaying modes are closed; there are modes with decay rates much less than  $\gamma$ .

Naturally, the localised stationary state can be entangled. The simplest example of the entangled states for the minimal localised states of the infinite square lattice of Fig. S5(a) up to the normalization factor is

$$|\Psi^{loc}\rangle = |\alpha\rangle_{j+1,k} |\alpha\rangle_{j+2,k} |\alpha\rangle_{j+2,k+1} |\alpha\rangle_{j+1,k+1} + |-\alpha\rangle_{j+1,k} |\alpha\rangle_{j+2,k} |-\alpha\rangle_{j+2,k+1} |\alpha\rangle_{j+1,k+1}$$

which for  $|\alpha| > 0$  is entangled since an averaging over any mode included in this equation gives a mixed state. Up to the normalization factor the reduced state of any three modes is given by

$$\rho_3 = |\psi_3^+\rangle \langle \psi_3^+| + |\psi_3^-\rangle \langle \psi_3^-| + e^{-2|\alpha|^2} (|\psi_3^+\rangle \langle \psi_3^-| + |\psi_3^-\rangle \langle \psi_3^+|),$$

where  $|\psi_3^\pm\rangle = |\pm\alpha\rangle_l \mp |\alpha\rangle_m \pm |\alpha\rangle_n$ , and indexes  $l, m, n$

number three modes remained after averaging over the fourth one.

Another example of the localised state is the state with just a single photon distributed over several lattice sites, such as

$$|\Psi^{loc}\rangle = \sum_{k \in \{n\}} (-1)^l |1\rangle_k, \quad (\text{S14})$$

where the index  $l$  numbers modes along the closed contour connecting all the sites belonging to the set  $\{n\}$  where the state is localised; the state  $|1\rangle_k$  corresponds to the photon in  $k$ -th mode and the vacuum in all other

modes. The same localisation regions as for the coherent modal states are possible for both the perfect and finite lattices. For example, the upper-left corner state of the lattice Fig. S5(a) is  $|\Psi^{loc}\rangle = 2|1\rangle_1 - |1\rangle_2 - |1\rangle_3$ . The states of Eq. (S14) are entangled. Amount of entanglement is proportional to the number of systems in the localised state. For example, the generalized Schmidt number for the state of Eq. (S14) is  $2(N - 1)$ ,  $N$  being the number of sites [27]. Notice that existence of the localised state Eq. (S14) points to possibility of dissipative compacton-like localisation in fermionic lattices, too.